ACS OMEGA

Open Access

This article is licensed under CC-BY-NC-ND 4.0

http://pubs.acs.org/journal/acsodf

Article

Comparative Pharmacokinetics and Tissue Distribution of Hexahydrocurcumin Following Intraperitoneal vs Oral Administration in Mice Using LC-MS/MS

Worawut Chaiyasaeng, Darunee Hongwiset,* Chainarong Tocharus, Baralee Punyawudho, Jiraporn Tocharus, Waraluck Chaichompoo, Pornchai Rojsitthisak, Wachirachai Pabuprapap, Boon-ek Yingyongnarongkul, and Apichart Suksamrarn

Cite This: *ACS Omega* 2024, 9, 41032−41042

Read Online

ACCESS | Metrics & More | Article Recommendations | Supporting Information

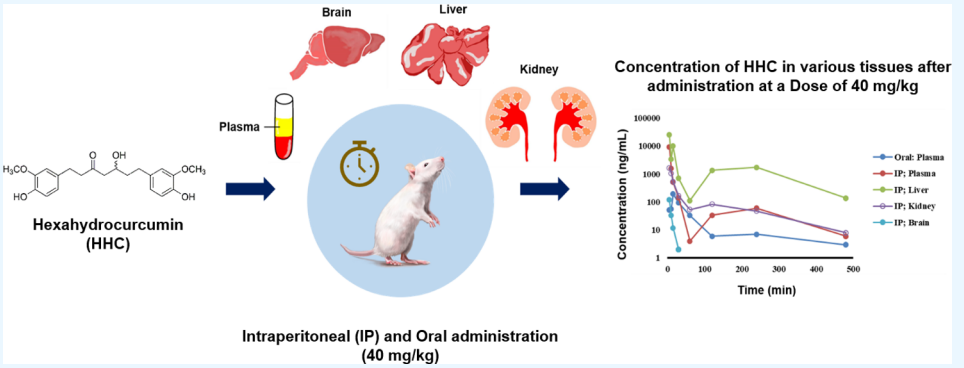

ABSTRACT: A liquid chromatography-tandem mass spectrometry (LC-MS/MS) method was developed and validated to determine hexahydrocurcumin (HHC) levels in mouse plasma, brain, liver, and kidneys using a negative ion mode electrospray ionization (ESI) source. Demonstrating a lower limit of quantification (LLOQ) of 5 ng/mL, the method showed excellent linearity across a concentration range of 5−500 ng/mL in all tested matrices. Precision evaluations reported a coefficient of variation (CV%) of less than 13.19% for both intraday and interday measurements, while accuracy ranged from 95.13 to 105.07% across all quality control levels. HHC extraction recovery was consistently observed between 70.18 and 93.28%, with a CV% deviation of less than 15%. In the pharmacokinetic evaluation of HHC in mice following a single intraperitoneal (IP) or oral administration, a noncompartment analysis was utilized. After IP administration (40 mg/kg), the C_{max} value was 47.90 times higher than that achieved via oral administration. Peak plasma concentrations were observed approximately 5 min post-IP and 15 min post-oral dosing. The observed half-lives after these administrations were approximately 1.52 and 2.17 h for IP and oral routes, respectively. Oral administration revealed a relative bioavailability of only 12.28% compared with the IP route. Furthermore, following IP administration, the half-life values in brain, liver, and kidney were not significantly different but more than the half-life value found in plasma. The liver and kidney exhibited the highest concentrations of HHC, while the brain showed the least, suggesting that the hydrophobic nature of HHC impedes its passage through the blood−brain barrier. This study is the first to provide detailed insights into the pharmacokinetics and tissue distribution characteristics of HHC following oral and IP administration in mice, setting the stage for further focus on HHC as a potential new drug candidate.

1. INTRODUCTION

Hexahydrocurcumin (HHC, Figure 1), recognized as a significant phase I metabolite of curcumin, is prevalent in both mice and humans.[1,2] From a structural viewpoint, HHC parallels curcumin, possessing identical phenolic groups, suggesting that it might manifest many of curcumin's known biological and pharmacological properties. However, HHC distinguishes itself in terms of stability; the absence of olefinic double bonds provides HHC with superior stability to curcumin, especially at a pH of 7.4.[3] In a diverse range of in vitro and in vivo studies, HHC has consistently displayed bioactivities that are either parallel to or exceeding those of curcumin. Notably, these biological activities include anti-oxidative,[4−8] anti-inflammatory,[7,9,10] antitumor,[11] cytotoxic,[12]

Received: July 17, 2024
Revised: September 7, 2024
Accepted: September 9, 2024
Published: September 19, 2024

© 2024 The Authors. Published by American Chemical Society

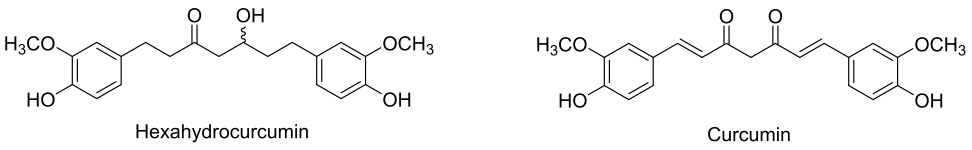

Figure 1. Chemical structures of hexahydrocurcumin (HHC) and curcumin.

and cardioprotective properties.[13] Some studies even emphasize HHC's superior bioactive prowess over curcumin, its metabolic precursor, particularly its antioxidant potential.[5,6] Delving deeper into its therapeutic attributes, oncological research highlights HHC's role in stifling the proliferation of human colon cancer cells, especially when synergistically combined with the chemotherapeutic agent 5-fluorouracil (5-FU). This combined therapeutic approach effectively curbed the viability of HT-29 cells via a profound down-regulation of COX-2 mRNA and protein expression, marking a decline in human colon cancer cell proliferation and an evident synergy in decreasing aberrant crypt foci (ACF) formation.[14,15] Our cardiovascular-focused investigations have revealed HHC's vasorelaxant properties, which induce relaxation in rat aortic rings by mitigating calcium ion concentrations.[16] Moreover, HHC's multifaceted role in neuroprotection has been recognized, with studies indicating its ability to shield the blood−brain barrier against cerebral ischemia/reperfusion-induced injuries, modulate tight junction proteins, reduce inflammation, and stave off the onset of brain edema.[17] HHC also mitigates dexamethasone-induced Alzheimer's disease-like symptoms by alleviating oxidative stress, inflammation, apoptosis, and improving memory deficits.[18,19] Building on this array of benefits, our recent findings highlight HHC's potential in hypertension management, accentuating its role in refining vascular function and reversing vascular remodeling.[19]

Although various pharmacological properties are explored, only limited information about the bioanalysis and pharmacokinetic study of HHC has been reported. The method validation of HHC in plasma, as one of the metabolites of curcumin, was reported by Jude et al.[20] However, the pharmacokinetic data of HHC in various mouse tissues still needs to be clarified, as this information is essential in the early stages of new drug development.[21] It provides a comprehensive understanding of how a drug is metabolized, distributed, and absorbed by an organism. Notably, many drug development stalls or failures can be attributed to unsatisfactory pharmacokinetic characteristics, such as reduced bioavailability or limited metabolic stability.[22] Existing research has extensively documented the pharmacokinetics of curcumin.[23−25] In animal studies, curcumin showed poor systemic bioavailability after administration.[26] For instance, after an IP dose of 0.1 g/kg was administered to mice, the peak plasma concentration of free curcumin reached only 2.25 μg/mL. The distribution of curcumin in tissues revealed levels of 26.90 μg/g in the liver and 7.51 μg/g in the kidneys, respectively. Notably, only trace amounts (0.41 μg/g) were detected in the brain at 1 h after administration.[27] When administered orally at a dosage of 500 mg/kg in rats, the maximum concentration (C_{max}) and the time taken to reach the maximum concentration (T_{max}) were 0.06 ± 0.01 μg/mL and 41.7 ± 5.4 min, respectively. The elimination half-life ($T_{1/2,\beta}$) was calculated to be 28.1 ± 5.6 min for curcumin (500 mg/kg, oral) and 44.5 ± 7.5 min for curcumin (10 mg/kg, intravenous). The oral bioavailability was estimated to be approximately 1%.[26] Furthermore, curcumin levels in tissues from rats that received oral curcumin (340 mg/kg) were examined, and the samples were analyzed at 20 min post-dose. The results indicated the presence of curcumin in plasma (16.1 ng/mL), liver (3671.8 ng/g), and kidneys (206.8 ng/g) following administration.[28]

Several instances of the intravenous administration of curcumin have been documented. Following intravenous curcumin administration (20 mg/kg) in mice, the pharmacokinetics and distribution of curcumin and its metabolites showed a rapid decrease in plasma concentration of curcumin with $T_{1/2,z}$ of 32.3 ± 10.8 min. The $AUC_{0-\infty}$ of curcumin (107.0 ± 18.3 mg·min/L) was approximately 17.8 times that of dihydrocurcumin (6.0 ± 1.2 mg·min/L) and 8.9 times that of tetrahydrocurcumin (THC) (12.0 ± 4.0 mg·min/L). Both curcumin and tetrahydrocurcumin were detectable in the liver. In the kidneys, curcumin and dihydrocurcumin were present. However, only curcumin was detected in the brain.[29] While extensive research has been conducted on the pharmacokinetics of curcumin, our knowledge regarding the pharmacokinetics of HHC after its administration remains notably limited,[20,30] and addressing this gap is crucial in the initial phases of drug development.

In this study, we aimed to develop and validate an liquid chromatography-tandem mass spectrometry (LC-MS/MS)-based method for HHC quantification, using butylparaben as an internal standard (IS), and to use this method to determine the pharmacokinetic profile of HHC after a single IP and oral administration in mice. Our investigation primarily focused on the concentration of HHC in plasma and its distribution in significant tissues, such as the brain, liver, and kidneys. A pivotal aspect of our research was assessing the relative bioavailability of HHC in mice. These findings are anticipated to provide valuable insights, enhancing the potential of HHC as a promising drug candidate.

2. RESULTS AND DISCUSSION

2.1. Method Development and Optimization. LC-MS/MS method was developed to quantify the HHC level in plasma, liver, kidney, and brain. Various extraction methods were tried in this study, not only solvent extraction but also protein precipitation with many solvents. The suitable sample preparation for the determination of HHC in plasma and brain was the solvent extraction with methyl *tert*-butyl ether (MTBE). Since kidney and liver samples were thicker, protein precipitation with acetone was added as the first step in the extraction method, followed by solvent extraction. Extraction recovery and matrix effects for all tissues were performed. The suitable internal standard was butylparaben, which showed high sensitivity and provided stable extraction recovery and proper retention time (RT). Negative mode showed higher sensitivity than positive mode in this study. To select the parent and daughter ions, the mass spectrum was scanned. The most sensitive mass transition was found as m/z 373→179 for

https://doi.org/10.1021/acsomega.4c06604
ACS Omega 2024, 9, 41032−41042

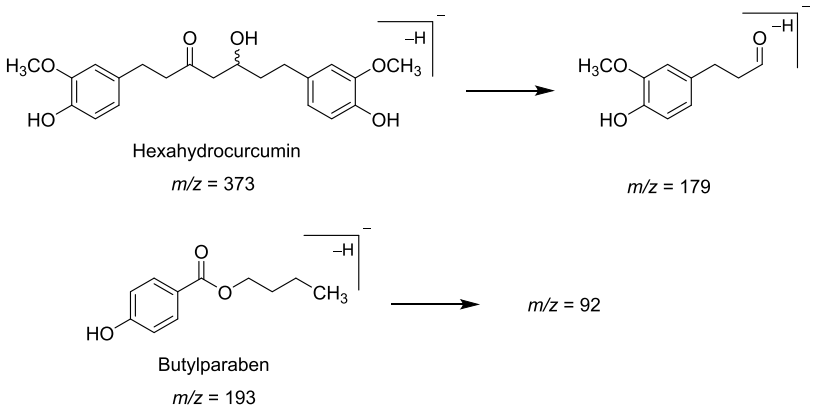

Figure 2. Proposed molecular ion of HHC and butylparaben (IS) and daughter ions.

Table 1. Regression Equations of HHC in All Matrix, R^2, Linear Range, LLOQ, and S/N Ratio[a]

matrix	regression equation	R^2	linear range (ng/mL)	LLOQ (ng/mL)	S/N ratio at LLOQ
plasma	$y = 1.7797 \times 10^{-3}x - 1.5662 \times 10^{-3}$	0.9979	5−500	5.00	23.40
liver	$y = 1.8441 \times 10^{-3}x + 5.7768 \times 10^{-4}$	0.9989			16.30
kidney	$y = 1.8325 \times 10^{-3}x - 1.183 \times 10^{-3}$	0.9955			13.20
brain	$y = 1.8497 \times 10^{-3}x - 8.725 \times 10^{-4}$	0.9970			28.70

[a]Acceptance criteria of LLOQ: accuracy within 80−120% of the nominal concentration; precision (CV%) ≤ 20%; signal-to-noise ratio (S/N) ≥ 5.

HHC and as m/z 193→92 for butylparaben. The proposed fragmentation is shown in Figure 2.

2.2. Method Validation. *2.2.1. System Suitability.* The system suitability demonstrated that the retention times of either HHC or butylparaben were approximately the same in all of the chromatograms. Their peaks were well separated without significant interference from any endogenous substance. Moreover, their peak area and peak area ratio showed coefficient of variation (CV%) within the acceptable range (Table S1, Supporting Information). Hence, it can be concluded that the resolution and reproducibility of the chromatographic system were adequate for the analysis of samples during the validation process.

2.2.2. Selectivity. The chromatograms of the solution of HHC (RT = 3.25 min) and butylparaben (RT = 5.58 min) are shown in Figure S1 (Supporting Information). HHC in plasma, brain, liver, and kidney showed peaks at retention times of 3.24, 3.22, 3.23, and 3.22 min, respectively (Table S2, Supporting Information). These retention times corresponded to the standard solution (RT = 3.25 min). Butylparaben showed a similar retention time at 5.49−5.58 min. In the blank mice plasma and tissue, no peak is shown at all retention time areas. Therefore, it could be concluded that the selectivity of HHC and butylparaben was demonstrated in this study (Figure 3).

2.2.3. Linearity of Calibration Curves and Lower Limit of Quantification (LLOQ). The calibration curve had a good linearity of HHC in the plasma concentration range from 5−500 ng/mL on three different days (Table S3, Supporting Information), where the established method can be seen to meet the requirements of the quantitative determination of HHC in pharmacokinetic studies. In addition, the calibration range of HHC in plasma, liver, kidney, and brain was from 5 to 500 ng/mL, and all calibration curves showed good linearity, with R^2 greater than 0.99 (Table 1). The representative calibration curves for the determination of HHC concentrations in mice plasma are shown in Figure S2. The lowest HHC level for quantification presented as LLOQ was 5 ng/mL in all matrices, with the signal-to-noise (S/N) ratio ranging from 13.20 to 28.70, accuracy of 83.10−111.93, and precision (CV%) of 5.32−13.19. Lower limits of detection from calculation for the limit of HHC in plasma, liver, kidney, and brain were 0.57, 1.08, 2.29, and 0.58 ng/mL, respectively.

2.2.4. Accuracy and Precision. The intraday and interday precision and accuracy of LLOQ (5 ng/mL) (n = 3) and QC samples at three concentration levels (15, 150, and 375 ng/mL) (n = 3) are summarized in Table 2. The accuracies for all tested concentrations were within ±7% of nominal, and both the within- and between-run precisions were acceptable. All of the results of the tested samples were within the acceptable criteria (accuracy (85−115%) and precision (CV ≤ 15%)).

2.2.5. Extraction Recovery and Matrix Effect. At different concentration levels, the mean recovery for HHC and IS in plasma, brain, liver, and kidney are summarized in Table 3. The extraction recovery of HHC in all matrices was 89.62% in plasma, 93.28% in brain, 72.60% in kidney, and 70.18% in liver. However, there is no acceptance criterion for recovery of HHC in kidney and liver since the recovery reproducibility is good enough to stay within the accuracy and precision acceptance criteria. In contrast, the extraction recovery of IS in all matrices was found in the range of 81.23−113.74%. The precision of all extractions was demonstrated with the CV with the acceptance criteria of ≤15%. Matrix effect values of HHC were 92.82% in plasma, 105.05% in brain, 86.50% in kidney, and 77.70% in liver. In comparison, matrix effect values of IS were found to be 121.57% in plasma, 117.24% in brain, 122.63% in kidney, and 103.45% in liver. The precision of all matrices was demonstrated with the CV with the acceptance criteria of ≤15%.

2.2.6. Stability. The stock solution stability of HHC and IS was studied after being kept in a freezer at −30 ± 10 °C for 20 days. Their accuracy was 106.15 and 101.80%, and their precision was 0.36 and 0.80%, respectively. So, these results indicate that both compounds were stable for at least 22 days at −30 ± 10 °C (Table 4). Moreover, long-term stability was studied to determine the stability of HHC in mice plasma

https://doi.org/10.1021/acsomega.4c06604
ACS Omega 2024, 9, 41032−41042

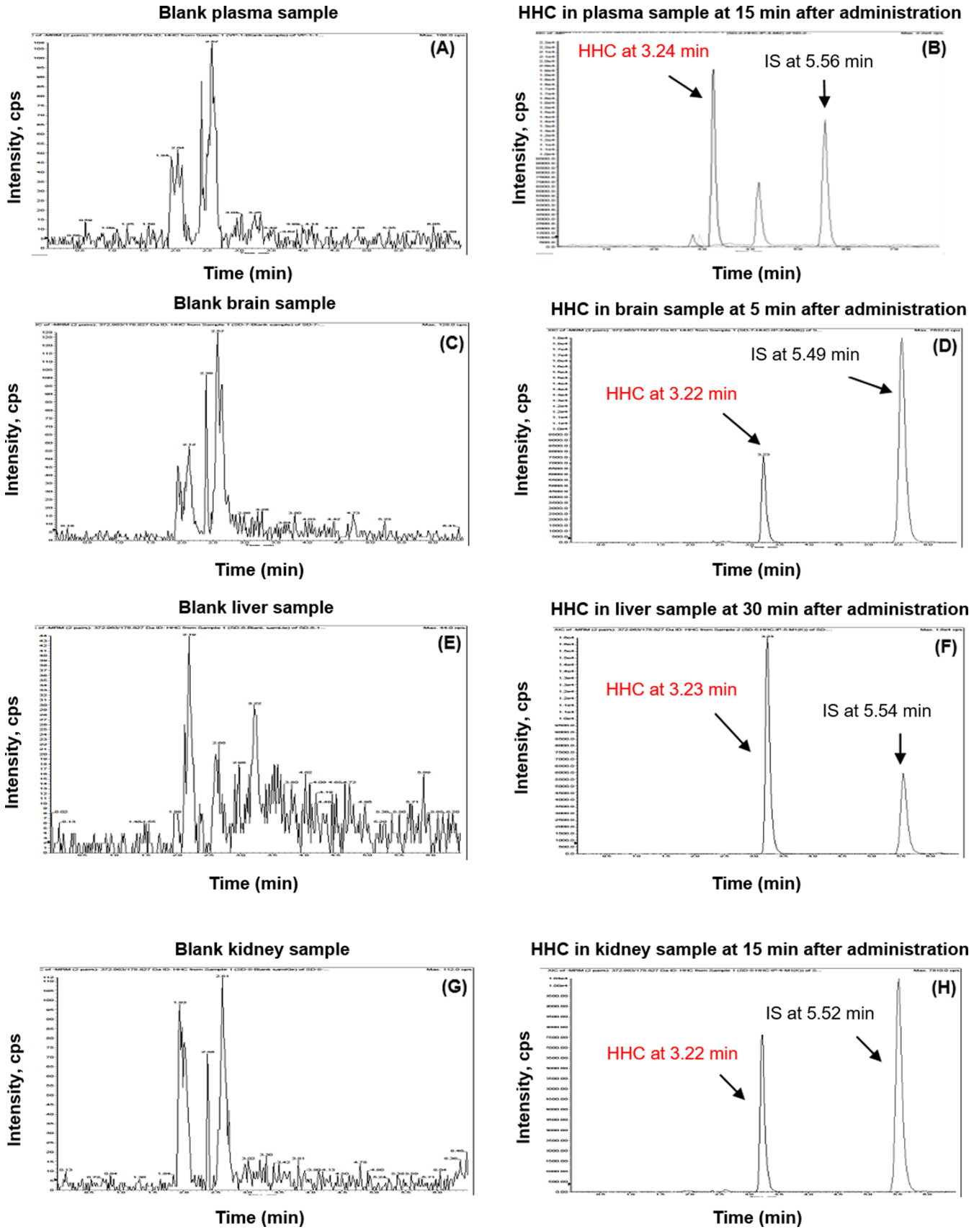

Figure 3. Exemplary chromatograms of blank and samples obtained after various time points of HHC administration from (A, B) plasma; (C, D) brain; (E, F) liver; and (G, H) kidney.

https://doi.org/10.1021/acsomega.4c06604
ACS Omega 2024, 9, 41032−41042

Table 2. Intraday and Interday Accuracy and Precision of LLOQ and QC Sample of HHC in Mice Plasma (Mean ± Standard Deviation (SD))

item	nominal conc. (ng/mL)	observed conc. (ng/mL)	accuracy (%)	precision (CV%)
accuracy and precision of LLOQ sample of HHC				
intra- and interday				
calibration curve: $y = 1.5341 \times 10^{-3}x - 1.8465 \times 10^{-4}$; $R^2 = 0.9959$				
intraday (n = 3)	5.00	5.30 ± 0.30	106.04	5.66
interday (n = 9)	5.00	4.97 ± 0.66	99.47	13.19
accuracy and precision of QC sample of HHC				
intraday				
calibration curve: $y = 1.5341 \times 10^{-3}x - 1.8465 \times 10^{-4}$; $R^2 = 0.9959$				
interday				
calibration curve day1: $y = 1.5341 \times 10^{-3}x - 1.8465 \times 10^{-4}$; $R^2 = 0.9959$				
calibration curve day2: $y = 1.6891 \times 10^{-3}x - 2.2302 \times 10^{-4}$; $R^2 = 0.9932$				
calibration curve day3: $y = 1.7797 \times 10^{-3}x - 1.5662 \times 10^{-3}$; $R^2 = 0.9979$				
intraday (n = 3)	15.00	14.80 ± 0.49	98.68	3.28
	150.00	157.60 ± 10.75	105.07	6.82
	375.00	382.78 ± 33.28	102.08	8.69
interday (n = 9)	15.00	14.39 ± 1.11	95.97	7.73
	150.00	143.38 ± 8.50	95.59	8.89
	375.00	356.74 ± 0.30	95.13	9.26

Table 3. Extraction Recovery and Matrix Effect of HHC and IS in Mice Plasma, Brain, Liver, and Kidney (Mean ± SD, n = 3)

	HHC		IS	
tissues (matrix)	accuracy (%)	precision (CV%)	accuracy (%)	precision (CV%)
extraction recovery				
plasma	89.62 ± 3.57	3.99	113.74 ± 8.64	7.59
brain	93.28 ± 6.07	6.51	112.24 ± 6.56	5.84
liver	70.18 ± 2.20	3.13	81.23 ± 3.03	3.73
kidney	72.60 ± 5.90	8.12	109.66 ± 6.87	6.26
matrix effect				
plasma	92.82 ± 2.75	2.97	121.57 ± 8.32	6.84
brain	105.05 ± 10.73	10.22	117.24 ± 3.20	2.73
liver	77.70 ± 6.32	8.14	103.45 ± 5.30	5.13
kidney	86.50 ± 0.06	0.07	122.63 ± 15.19	12.39

Table 4. Stock Solution Stability of HHC and IS at −30 ± 10 °C for 22 days (Mean ± SD, n = 3)

analyte (nominal conc., ng/mL)	observed conc. (ng/mL)	accuracy (%)	precision (CV%)
fresh			
HHC (375.00)	375.00 ± 18.19	100	4.85
IS (110.10)	110.10 ± 1.38	100	1.25
stock stability for 22 days			
HHC (375.00)	398.08 ± 1.45	106.15	0.36
IS (110.10)	112.08 ± 0.90	101.80	0.80

under storage at −30 ± 10 °C for 20 days and analytical conditions. The stability of HHC in mice plasma is shown in Table 5. The results showed that HHC in plasma samples was stable after storage at −30 ± 10 °C for 20 days. However, stability on other tissues is pivotal for the accurate interpretation of drug concentration over time and is a critical component of method validation. This is an area for future investigation, which is crucial for a full understanding of the pharmacokinetics of HHC.

2.2.7. Dilution Effect. Dilution of the plasma sample 20 times was studied. The result showed an accuracy of 87.10%

Table 5. Long-Term Stability of HHC in Plasma at −30 ± 10 °C for 20 days (Mean ± SD, n = 3)

analyte (nominal conc., ng/mL)	observed conc. (ng/mL)	accuracy (%)	precision (CV%)
fresh			
LQC (15.00)	12.85 ± 0.31	86.66	2.38
HQC (375.00)	346.27 ± 17.85	92.34	5.15
long-term stability for 20 days			
LQC (15.00)	13.54 ± 1.03	90.27	7.61
HQC (375.00)	355.53 ± 34.51	94.81	9.71

and a precision of 3.13% (Table 6). Therefore, it showed the dilution integrity of HHC 20 times. The optimized method

Table 6. Dilution Integrity of HHC in Plasma

	test sample-HHC (7500.00 ng/mL)		
	test sample-HHC 375 ng/mL (dilution factor 20×)		
sample no.	estimated conc. (ng/mL)	estimated conc. (before dilution) (ng/mL)	accuracy (%)
1	333.02	6660.40	88.81
2	332.00	6640.00	88.53
3	314.81	6296.20	83.95
mean	326.61	6532.20	87.10
SD	10.23	204.64	2.73
CV (%)	3.13	3.13	3.13
evaluation			passed

was validated to guarantee reliable determination results for HHC and was successfully applied to the pharmacokinetic study after both IP and oral administration in mice.

2.3. Pharmacokinetics and Tissue Distribution Study of HHC. In the pharmacokinetics and distribution study, HHC concentrations were measured in liver, kidney, brain, and plasma within 24 h after administration to mice. The concentration−time profiles of HHC in the logarithm scale are shown in Figure 4. The main pharmacokinetic parameters (PK), based on noncompartment analysis, are summarized in Table 7. The results showed that HHC was widely distributed in these tissues and plasma, reaching a maximum level within

https://doi.org/10.1021/acsomega.4c06604
ACS Omega 2024, 9, 41032−41042

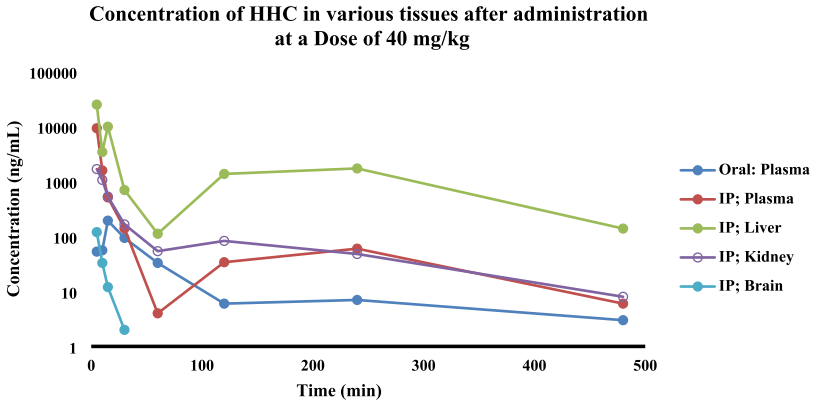

Figure 4. Mean concentration−time profiles of HHC in logarithm scale at a dose of 40 mg/kg after IP and oral administration to mice (n = 4); excluded HHC in the brain after IP was n = 3. The samples were collected at specific intervals: 30 min before dosing and subsequently at 5, 10, 15, 30, 60, 120, 240, and 480 min post administration, and 1440 min post administration was not shown.

Table 7. Noncompartmental Pharmacokinetic Parameter of HHC at Dose 40 mg/kg after Oral/IP Administration in Mice (n = 4)

PK parameters	AUC_{0-t} (ng·min/mL)	$AUC_{0-\infty}$ (ng·min/mL)	MRT_{0-t} (min)	$MRT_{0-\infty}$ (min)	$T_{1/2}$ (min)	C_{max} (ng/mL)	T_{max} (min)
oral-plasma	7610.4 ± 1906.9	8545.1 ± 2044.9	96.8 ± 29.0	154.7 ± 49.6	130.2 ± 32.1	194.2 ± 43.5	15.0 ± 0.0
IP-plasma	61 967.7 ± 1759.6	62 838.2 ± 16 997.4	42.5 ± 28.7	52.5 ± 28.3	91.2 ± 15.3	9299.0 ± 4286.9	5.0 ± 0.0
IP-liver	572 497.7 ± 270 586.6	576 329.6 ± 272 103.4	156.2 ± 39.4	160.1 ± 35.8	104.5 ± 25.8	25 043.3 ± 12 061.5	5.0 ± 0.0
IP-kidney	37 213.4 ± 12 705.8	38 922.3 ± 14 659.8	96.3 ± 20.6	116.5 ± 37.4	101.7 ± 37.4	1703.0 ± 897.2	6.3 ± 2.5
IP-brain	1120.8 ± 439.8	1267.5 ± 507.2	62.9 ± 64.2	122.5 ± 91.9	106.1 ± 58.8	120.2 ± 54.1	5.0 ± 0.0

Area under the concentration−time curve (AUC) computed from time zero to the time of the last positive t value (AUC_{0-t}); AUC from time zero extrapolated to infinity ($AUC_{0-\infty}$); mean residence time when the drug concentration is based on values up to and including the last measured concentration (MRT_{0-t}); MRT from time zero extrapolated to infinity ($MRT_{0-\infty}$); elimination half-life ($T_{1/2}$); maximum observed drug concentration (C_{max}); and time of maximum concentration (T_{max}). All of the HHC PK values are listed as the mean value ± SD. Each mean ± SD (n = 4) is represented by each point.

5−15 min, and was rarely detected after 1 h. After IP administration of HHC 40 mg/kg to mice, the highest concentration of HHC in the liver, brain, and plasma was found at 5 min, except in the kidney found at 6.30 min with a C_{max} of 25 043.3 ± 12 061.5, 120.2 ± 54.1, 9299.0 ± 4286.9, and 1703.0 ± 897.2 ng/mL, respectively. Interestingly, following intraperitoneal (IP) injection, we detected two distinct peaks of HHC levels in the plasma and liver. While the exact reasons for the occurrence of the second peak are not known, we hypothesize that the presence of a second peak in the plasma could be attributable to the hepatic recirculation of HHC. Drug absorption via the IP route to the liver occurs through diffusion across the capillaries and then enters the portal vein. Rediffusion and fluctuation of peritoneal blood flow to the liver could be the potential explanation for this phenomenon.[31] After oral administration of HHC 40 mg/kg to mice, the highest concentration in plasma was found at 15 min with a C_{max} of 194.2 ± 43.5 ng/mL. Prior researches have demonstrated that curcumin has a limited oral bioavailability, leading to minimal or undetectable levels of the compound in the plasma upon oral administration.[32,33] However, HHC appears to enhance solubility. The results of our study indicate that the relative oral bioavailability of HHC is low. Specifically, the percent relative bioavailability of HHC, calculated by the ratio of AUC_{0-t} after oral administration to the AUC_{0-t} following IP administration, was 12.28%.

After IP administration of HHC at 40 mg/kg, the C_{max} value was 47.9 times higher than that in the oral dosage regimen. The half-life of HHC in plasma after IP and oral administrations was about 91.2 min (1.52 h) and 130.2 min (2.17 h), respectively, demonstrating rapid elimination of HHC after IP administration compared to oral administration. Although the HHC half-lives in plasma, brain, liver, and kidney were comparable after IP administrations of HHC, the half-life in the brain tended to be longer than that in the liver, kidney, and plasma. This indicates that the rate of redistribution was the slowest in the brain, as opposed to the liver and kidney. The half-life of HHC, as determined in our study, was found to be longer than the half-life of curcumin in rats, which was 32.7 min after oral administration.[34]

The tissue distribution study revealed that following IP administration of HHC, a substantial amount of HHC was distributed to both the liver and kidney. Our investigation found a small quantity of HHC in the brain, which aligns with a previous pharmacokinetic study that observed the lowest concentration of curcumin in the brain.[27] This may be attributed to the high hydrophilic characteristics of both curcumin and HHC. Consequently, it has a reduced ability to cross the blood−brain barrier. However, one mouse showed a noticeably rapid decrease in HHC concentrations in the brain compared with the other mice, rendering it impossible to calculate the pharmacokinetic parameters for that mouse. Consequently, the pharmacokinetic parameters of HHC in the brain were determined by using data from the remaining three mice. To the best of our knowledge, while previous studies have focused on the pharmacokinetics of HHC following oral administration in plasma,[20] this study is the first to present comprehensive pharmacokinetic data of HHC across mouse tissues. This information is crucial for advancing the early stages of drug development.

https://doi.org/10.1021/acsomega.4c06604
ACS Omega 2024, 9, 41032−41042

3. CONCLUSIONS

In this work, a highly sensitive and specific LC-MS/MS method for the quantitation of hexahydrocurcumin (HHC) in mice plasma, liver, kidney, and brain has been developed. Moreover, this method was successfully applied to pharmacokinetic and tissue distribution studies in mice. The HHC concentrations in plasma, liver, kidney, and brain after IP administration and the HHC concentration in plasma after oral administration were estimated. For the HHC concentration in plasma, the maximum concentration was found within 5 and 15 min after IP and oral administration, respectively, the half-life of which was about 1.52 and 2.17 h, respectively. The percent relative bioavailability after oral administration was 12.28 compared to that after IP administration. In terms of tissue distribution, HHC was highly and rapidly distributed to the liver and kidney, whereas the lowest concentration of HHC was found in the brain, which could be due to the high hydrophilic property of the compound. It was, therefore, difficult for HHC to cross the blood−brain barrier. The results from this study provide initial evidence for interspecies dose extrapolation to estimate the probable pharmacokinetic properties in humans. This knowledge is crucial for the development of HHC as a potential drug candidate.

4. MATERIALS AND METHODS

4.1. Chemicals and Reagents. HHC was synthesized from curcumin, which was obtained from *Curcuma longa* rhizomes by our published method.[18,35] Briefly, curcumin was dissolved in ethanol and was hydrogenated with palladium on charcoal as a catalyst for 8 h to yield the hydrogenated products, which were separated by column chromatography (silica gel, with dichloromethane/methanol as eluent) to give HHC (84%) and octahydrocurcumin (8%). The spectroscopic (^{1}H and ^{13}C NMR and mass spectra) data of the isolated HHC were consistent with those reported in the literature.[18] HHC was obtained with a purity of >97.0% (by high-performance liquid chromatography (HPLC) analysis). Butylparaben, with a purity of 99.6% and used as the internal standard (IS), was purchased from Alfa Aesar (Lancashire, U.K.). Methanol and acetonitrile (HPLC grade) were obtained from Avantor Performance Materials (J.T. Baker, Center Valley, PA). Sodium acetate trihydrate, hydrochloric acid, methyl *tert*-butyl ether (MTBE) (AR grade), water, and acetone (HPLC grade) were supplied by RCI Labscan Group (Bangkok, Thailand). Acetic acid (AR grade) was obtained from Fisher Scientific UK Ltd. (Leics, U.K.). Formic Acid (AR grade) was acquired from Merck KGaA (Darmstadt, Germany).

4.2. Animals. Eighty male mice weighing 18−22 g were obtained from Nomura Siam International Company Ltd. (Bangkok, Thailand) and allowed a week for environment adaptation before the experiment. All mice were housed in an environment maintained at 25 ± 1 °C under a 12-h light−dark cycle, with access to food and water ad libitum.

Sample collection was performed after IP or Oral Administration of 40 mg/kg HHC, which was an effective dose for improvement of cognitive function, as shown in our previous results.[17−19] All experiments in this study were approved by the Institutional Animal Care and Use Committee at the Faculty of Medicine, Chiang Mai University, in compliance with National Institutes of Health guidelines (Permit No. 44/2563).

Briefly, HHC was prepared at a concentration of 40 mg/kg of body weight by dissolving it in 0.1% dimethyl sulfoxide (DMSO), followed by dilution in 1% hydroxyethyl cellulose. The solution volume was adjusted based on the mouse's body weight (1 g BW: 10 μL solution). Eighty mice were divided into two main sets: one for IP administration and the other for administration via oral gavage under veterinary supervision (oral administration). Within each set, mice were further divided into ten groups, each containing four mice.

Blood samples were collected at specific intervals: 30 min before dosing and subsequently at 5, 10, 15, and 30 min, 1, 2, 4, 8, and 24 h post administration. After the mouse was anesthetized, the thoracic cavity was opened, and the blood samples were collected from the left ventricle of the heart. The samples were then stored in vacuum blood tubes coated with ethylenediaminetetraacetic acid (EDTA) at 4 °C. Samples were then centrifuged at 4000 rpm for 10 min at 4 °C. The resulting plasma was stored at −30 ± 10 °C for subsequent analysis.

For the distribution study, tissues from the liver, kidney, and brain were procured. These tissues were homogenized in phosphate-buffered saline (PBS) at a 1:10 (w/w) ratio, vortexed for 5 min at 1500 rpm, and then stored at −30 ± 10 °C until analysis.

4.3. Chromatography and Mass Spectrometry Conditions. Analyses were performed using an Agilent 1260 system (Agilent, CA). For the separation of HHC and IS, a 5 μL sample was injected into the system. Separation occurred on a Mightysil RP-18 GP column (4.6 mm × 150 mm, 5 μm, Kanto Inc., Japan), paired with a Mightysil RP-18 guard column (4.0 mm × 10 mm, 5 μm, Thermo Scientific). Isocratic elution was employed using a mobile phase consisting of acetonitrile and 0.1% formic acid in a 65:35 (v/v) ratio. The mobile phase was maintained at a temperature of 35 °C, with a flow rate of 0.6 mL/min. The total run time for each analysis was 8 min.

Mass spectrometric measurements were conducted using the API 3200 system (AB Sciex, Singapore), an integrated triple quadrupole mass spectrometer. The electrospray ionization (ESI) source was set to operate in the negative ion mode. The specific detector parameters used for the analysis of HHC and IS in plasma, liver, kidney, and brain are detailed in Table S4 (Supporting Information). Quantification relied on the multiple reaction monitoring (MRM) method, targeting Q1/Q3 *m*/*z* values of 372.963/178.827 for HHC and 192.852/91.940 for IS.

4.4. Preparation of Standard Solutions. Stock solutions for HHC and IS were prepared by dissolving their respective standards in methanol to obtain concentrations of 500 and 1000 μg/mL, respectively. Separate stock solutions were prepared for calibration standards and quality control (QC) samples and were stored at −30 ± 10 °C. For the calibration curves, the HHC stock solution was diluted with blank plasma and tissue to achieve concentrations ranging from 5 to 500 ng/mL, specifically at 5, 10, 50, 100, 200, 300, 400, and 500 ng/mL. For QC purposes, HHC samples were prepared at concentrations of 15, 150, and 375 ng/mL. Concurrently, the IS stock solution was diluted in methanol to obtain a 1.1 μg/mL working solution. These working solutions, similar to the stock solutions, were kept at −30 ± 10 °C.

4.5. Preparation of Biological Samples. *4.5.1. Plasma and Brain Extraction.* For plasma and brain extraction, 10 μL of butylparaben, 50 μL of acetate buffer (pH 5.0), 50 μL of

https://doi.org/10.1021/acsomega.4c06604
ACS Omega 2024, 9, 41032−41042

ascorbic acid (200 mg/mL), and 50 μL of 0.1 N HCl were added into 100 μL of plasma or brain sample. Next, the mixture was shaken at 2500 rpm for 20 min. Then, 2.5 mL of methyl *tert*-butyl ether (MTBE) was added, mixed with a shaker, and centrifuged at 3500 rpm and 4 °C for 3 min. After the sample was separated, 2.0 mL of supernatant was carefully transferred to a new tube and evaporated under nitrogen gas at 0.5 psi and 25 °C for 15 min. Subsequently, the residue was reconstituted in 80 μL of mobile phase and mixed. After centrifugation at 3500 rpm for 10 min, 5 μL of each aliquot was injected into the LC-MS/MS system for analysis.

4.5.2. Kidney Extraction. For kidney extraction, 10 μL of butylparaben, 50 μL of acetate buffer (pH 5.0), 50 μL of ascorbic acid (200 mg/mL), 50 μL of 0.1 N HCl, and 200 μL of acetone were added into 100 μL of the kidney sample. Next, the mixture was mixed with a shaker at 2500 rpm for 20 min and centrifuged at 10,900 rpm for 10 min. All of the supernatant was collected, and then 4.8 mL of MTBE was added into the sample and mixed using a shaker at 2500 rpm for 20 min before centrifuging at 3500 rpm and 4 °C for 3 min. Subsequently, 4.5 mL of the supernatant was transferred into another test tube and evaporated under nitrogen gas at 0.5 psi and 25 °C for 20 min. Finally, the residue was reconstituted in 75 μL of the mobile phase and mixed. After centrifugation at 3500 rpm for 10 min, 5 μL of each aliquot was injected into the LC-MS/MS system for analysis.

4.5.3. Liver Extraction. For liver extraction, 20 μL of butylparaben, 100 μL of acetate buffer (pH 5.0), 100 μL of ascorbic acid (200 mg/mL), 100 μL of 0.1 N HCl, and 400 μL of acetone were added into 200 μL of the liver. Next, the mixture was mixed at 2000 rpm for 15 min and centrifuged at 10,900 rpm for 10 min. All of the supernatant was collected, and then 2.0 mL of MTBE was pipetted into the sample, mixed using a shaker at 2500 rpm for 20 min again, and centrifuged at 3500 rpm and 3 °C for 3 min. Subsequently, 1.8 mL of the supernatant was transferred into a new test tube and evaporated under nitrogen gas at 0.5 psi and 25 °C for 20 min. Finally, the residue was reconstituted in 75 μL of the mobile phase and mixed. After centrifugation at 3500 rpm for 10 min, 5 μL of each aliquot was injected into the LC-MS/MS system for analysis.

4.6. Method Validation. The method for quantifying HHC in plasma, liver, kidney, and brain was validated by using butylparaben as the preferred internal standard. The validation covers various parameters, including selectivity, matrix effect, LLOQ, calibration curve, precision, accuracy, extraction recovery, dilution integrity, and stability. This validation was in alignment with the acceptance criteria established by the FDA guidance on bioanalytical methods validation (US FDA 2018).[36]

4.6.1. System Suitability. The suitability of an analytical method was evaluated by comparing the retention times of the analytical peaks (HHC and IS) between blank samples from each matrix and samples spiked with either HHC or IS. The CV for the peak area, retention time, and peak area ratio was assessed using a criterion of ≤6.0% as the acceptable threshold.

4.6.2. Selectivity. Selectivity was assessed by comparing the retention of HHC and IS analytical peaks between the blank sample of each matrix and the analyte or spiked standard sample.

4.6.3. Linearity of Calibration Curves and LLOQ. The calibration range of HHC across plasma, liver, kidney, and brain samples was established between 5 and 500 ng/mL (n = 3). Calibration curves were constructed by plotting the peak area of the analyte against that of the internal standard relative to their respective concentrations. The correlation of determination (R^2) was calculated using weighted least-squares regression ($1/X^2$). The goodness-of-fit of the calibration curves was denoted by R^2. Precision was expressed using CV, while recovery (%) indicated accuracy. For each nominal concentration value in the calibration curves, the back-calculated concentrations should exhibit accuracy within ±15% and a precision of ≤15%. The LLOQ, indicating the minimum concentration of the calibration curve, should exhibit both accuracy and precision of ±20 and ≤20%, respectively. Additionally, a signal-to-noise ratio (S/N) of ≥5 is required.

4.6.4. Accuracy and Precision. The precision and accuracy of HHC were explored using three replicates at LLOQ and three QC sample concentration levels across 3 days. Concentrations were calculated from daily linear regression equations. Set standards for intraday and interday precision were established, along with accuracy requirements. For both intraday and interday measurements, the accuracy and precision of the LLOQ samples should remain within ±20% and not exceed ≤20%, respectively. Additionally, the precision should be within 15%, and the accuracy must not exceed ±15% at three QC levels.

4.6.5. Extraction Recovery and Matrix Effect. The recovery of HHC and IS was determined by comparing their peak area responses after extracting from the matrix sample to the response of the solution (n = 3). The matrix effect was evaluated by calculating the ratio of the peak area with the matrix present to the peak area without the matrix (n = 3). The acceptance criteria should ensure precision and accuracy values of ≤15% and within ±15% of the nominal concentrations, respectively.

4.6.6. Stability. To assess the stability of HHC and IS stock solutions, they were diluted with methanol to concentrations of 375 and 110 ng/mL, respectively (n = 3). These solutions, stored at −30 ± 10 °C for 22 days, were subsequently analyzed, and their peak responses were compared with those from freshly prepared stock solutions. The long-term stability of HHC was assessed at concentrations of 15 and 375 ng/mL in plasma (n = 3), which were stored at −30 ± 10 °C for 20 days. All results from these stability tests were compared to the nominal concentrations, accepting that precision should be within 15% and accuracy must not exceed ±15% of the nominal concentrations.

4.6.7. Dilution Effect. To ensure that the dilution with blank mouse plasma did not influence the final concentration, the dilution effect was evaluated. Triplicate samples of HHC spiked mice plasma, initially prepared at 7500 ng/mL, underwent a 20-fold dilution with blank mouse plasma. The dilution was deemed satisfactory if the assay results maintained accuracy with a recovery of ±15% and precision with CV% of ≤15%.

4.7. Application to Pharmacokinetic Study. The pharmacokinetics of HHC following oral and IP administration were assessed using data derived from bioanalysis. Analysis was conducted using standard noncompartmental methods with Phoenix WinNonlin, Version 8.0 software (Pharsight Corporation, St. Louis, MO). The bioavailability (F) of HHC after oral administration was determined based on eq 1:

https://doi.org/10.1021/acsomega.4c06604
ACS Omega 2024, 9, 41032−41042

$$F\ (\%) = \left(\frac{\mathrm{AUC_{oral}} \times \mathrm{dose_{ip}}}{\mathrm{AUC_{ip}} \times \mathrm{dose_{oral}}}\right) \times 100 \quad (1)$$

■ ASSOCIATED CONTENT

Supporting Information

The Supporting Information is available free of charge at https://pubs.acs.org/doi/10.1021/acsomega.4c06604.

Exemplary chromatograms of HHC and butylparaben solutions (Figure S1); representative calibration curve for determination of HHC concentrations in mice plasma (Figure S2); system suitability results of HHC in solution (Table S1); retention time of HHC and butylparaben (IS) (Table S2); accuracy and precision of back-calculated concentrations of calibration standards for HHC in plasma quantification (Table S3); detector and compound parameters of HHC analysis in plasma, liver, kidney and brain (Table S4) (PDF)

■ AUTHOR INFORMATION

Corresponding Author

Darunee Hongwiset − *Department of Pharmaceutical Sciences, Faculty of Pharmacy, Chiang Mai University, Chiang Mai 50200, Thailand;* orcid.org/0000-0002-7043-2867; Email: darunee.h@cmu.ac.th

Authors

Worawut Chaiyasaeng − *Department of Chemistry and Center of Excellence for Innovation in Chemistry, Faculty of Science, Ramkhamhaeng University, Bangkok 10240, Thailand*

Chainarong Tocharus − *Department of Anatomy, Faculty of Medicine, Chiang Mai University, Chiang Mai 50200, Thailand*

Baralee Punyawudho − *Department of Pharmaceutical Care, Faculty of Pharmacy, Chiang Mai University, Chiang Mai 50200, Thailand*

Jiraporn Tocharus − *Department of Physiology, Faculty of Medicine, Chiang Mai University, Chiang Mai 50200, Thailand*

Waraluck Chaichompoo − *Department of Chemistry and Center of Excellence for Innovation in Chemistry, Faculty of Science, Ramkhamhaeng University, Bangkok 10240, Thailand*

Pornchai Rojsitthisak − *Department of Food and Pharmaceutical Chemistry, Faculty of Pharmaceutical Sciences, Chulalongkorn University, Bangkok 10330, Thailand; Center of Excellence in Natural Products for Ageing and Chronic Diseases, Chulalongkorn University, Bangkok 10330, Thailand;* orcid.org/0000-0003-1391-6993

Wachirachai Pabuprapap − *Department of Chemistry and Center of Excellence for Innovation in Chemistry, Faculty of Science, Ramkhamhaeng University, Bangkok 10240, Thailand;* orcid.org/0000-0001-6445-7550

Boon-ek Yingyongnarongkul − *Department of Chemistry and Center of Excellence for Innovation in Chemistry, Faculty of Science, Ramkhamhaeng University, Bangkok 10240, Thailand;* orcid.org/0000-0002-9513-7282

Apichart Suksamrarn − *Department of Chemistry and Center of Excellence for Innovation in Chemistry, Faculty of Science, Ramkhamhaeng University, Bangkok 10240, Thailand;* orcid.org/0000-0001-8919-3555

Complete contact information is available at: https://pubs.acs.org/10.1021/acsomega.4c06604

Author Contributions

Conceptualization, D.H., C.T., B.P., and A.S.; methodology, C.T., D.H., and Wo.C.; investigation and data collection, Wo.C., D.H., J.T., Wa.C., P.R., W.P., and B.-e.Y.; data curation, C.T., D.H., and Wo.C.; formal analysis, D.H. and Wo.C.; software, D.H.; validation, D.H. and Wo.C.; writing—original draft, D.H. and Wo.C.; writing—review and editing, C.T., B.P., J.T., Wa.C., P.R., W.P., B.-e.Y., and A.S.; project administration and funding acquisition, A.S. All authors have read and agreed to the final version of the manuscript.

Funding

This work was supported by The Thailand Research Fund (TRF, grant No. DBG 6180030).

Notes

The authors declare no competing financial interest.

During the preparation of this work, the authors used ChatGPT 4.0 in order to improve language and readability. After using this tool, the authors reviewed and edited the content as needed, and they take full responsibility for the content of the publication.

■ ACKNOWLEDGMENTS

The authors would like to thank the staffs of Pharmacy Service Center (PSC), Faculty of Pharmacy, Chiang Mai University, especially Siriluk Sangsrijan, Saowarunee Sangsrijan, Kunthawat Siangwong and Akharapon Saiboukham for their helpful analytical support. Support from the Center of Excellence for Innovation in Chemistry, Ministry of Higher Education, Science, Research and Innovation is gratefully acknowledged.

■ ABBREVIATIONS

AUC	area under concentration−time curve
C_{max}	maximum concentration
CV	coefficient of variation
ESI	electrospray ionization
F	bioavailability
HHC	hexahydrocurcumin
HPLC	high-performance liquid chromatography
IP	intraperitoneal
IS	internal standard
LC-MS/MS	liquid chromatography-tandem mass spectrometry
LLOQ	lower limit of quantification
PK	pharmacokinetics
QC	quality control
SD	standard deviation
S/N	signal-to-noise ratio
$T_{1/2}$	half-life
T_{max}	time to reach C_{max}
R^2	correlation of determination
RT	retention time

■ REFERENCES

(1) Anand, P.; Thomas, S. G.; Kunnumakkaram, A. B.; Sundaram, C.; Harikumar, K. B.; Sung, B.; Tharakan, S. T.; Misra, K.; Priyadarsini, I. K.; Rajasekharan, K. N.; Aggarwal, B. B. Biological

activities of curcumin and its analogues (Congeners) made by man and Mother Nature. *Biochem. Pharmacol.* **2008**, *76* (11), 1590−1611.
(2) Holder, G. M.; Plummer, J. L.; Ryan, A. J. The metabolism and excretion of curcumin (1, 7-bis-(4-hydroxy-3-methoxyphenyl)-1, 6-heptadiene-3, 5-dione) in the rat. *Xenobiotica* **1978**, *8* (12), 761−768.
(3) Dempe, J. S.; Scheerle, R. K.; Pfeiffer, E.; Metzler, M. Metabolism and permeability of curcumin in cultured Caco-2 cells. *Mol. Nutr. Food Res.* **2013**, *57* (9), 1543−1549.
(4) Chen, W. F.; Deng, S. L.; Zhou, B.; Yang, L.; Liu, Z. L. Curcumin and its analogues as potent inhibitors of low density lipoprotein oxidation: H-atom abstraction from the phenolic groups and possible involvement of the 4-hydroxy-3-methoxyphenyl groups. *Free Radical Biol. Med.* **2006**, *40* (3), 526−535.
(5) Somparn, P.; Phisalaphong, C.; Nakornchai, S.; Unchern, S.; Morales, N. P. Comparative antioxidant activities of curcumin and its demethoxy and hydrogenated derivatives. *Biol. Pharm. Bull.* **2007**, *30* (1), 74−78.
(6) Deters, M.; Knochenwefel, H.; Lindhorst, D.; Koal, T.; Meyer, H. H.; Hänsel, W.; Resch, K.; Kaever, V. Different curcuminoids inhibit T-lymphocyte proliferation independently of their radical scavenging activities. *Pharm. Res.* **2008**, *25* (8), 1822−1827.
(7) Li, F.; Nitteranon, V.; Tang, X.; Liang, J.; Zhang, G.; Parkin, K. L.; Hu, Q. In vitro antioxidant and anti-inflammatory activities of 1-dehydro-[6]-gingerdione, 6-shogaol, 6-dehydroshogaol and hexahydrocurcumin. *Food Chem.* **2012**, *135* (2), 332−337.
(8) Morales, N. P.; Sirijaroonwong, S.; Yamanont, P.; Phisalaphong, C. Electron paramagnetic resonance study of the free radical scavenging capacity of curcumin and its demethoxy and hydrogenated derivatives. *Biol. Pharm. Bull.* **2015**, *38* (10), 1478−1483.
(9) Pan, M. H.; Lin-Shiau, S. Y.; Lin, J. K. Comparative studies on the suppression of nitric oxide synthase by curcumin and its hydrogenated metabolites through down-regulation of IκB kinase and NFκB activation in macrophages. *Biochem. Pharmacol.* **2000**, *60* (11), 1665−1676.
(10) Lee, S. L.; Huang, W. J.; Lin, W. W.; Lee, S. S.; Chen, C. H. Preparation and anti-inflammatory activities of diarylheptanoid and diarylheptylamine analogs. *Bioorg. Med. Chem.* **2005**, *13* (22), 6175−6181.
(11) Kuo, C. N.; Chen, C. H.; Chen, S. N.; Huang, J. C.; Lai, L. J.; Lai, C. H.; Hung, C. H.; Lee, C. H.; Chen, C. Y. Anti-angiogenic effect of hexahydrocurcumin in rat corneal neovascularization. *Int. Ophthalmol.* **2018**, *38* (2), 747−756.
(12) Chen, C. Y.; Yang, W. L.; Kuo, S. Y. Cytotoxic activity and cell cycle analysis of hexahydrocurcumin on SW 480 human colorectal cancer cells. *Nat. Prod. Commun.* **2011**, *6* (11), 1671−1672.
(13) Dong, H. P.; Yang, R. C.; Chunag, I. C.; Huang, L. J.; Li, H. T.; Chen, H. L.; Chen, C. Y. Inhibitory effect of hexahydrocurcumin on human platelet aggregation. *Nat. Prod. Commun.* **2012**, *7* (7), 883−884.
(14) Srimuangwong, K.; Tocharus, C.; Chintana, P. Y.; Suksamrarn, A.; Tocharus, J. Hexahydrocurcumin enhances inhibitory effect of 5-fluorouracil on HT-29 human colon cancer cells. *World J. Gastroenterol.* **2012**, *18* (19), 2383−2389.
(15) Srimuangwong, K.; Tocharus, C.; Tocharus, J.; Suksamrarn, A.; Chintana, P. Y. Effects of hexahydrocurcumin in combination with 5-fluorouracil on dimethylhydrazine-induced colon cancer in rats. *World J. Gastroenterol.* **2012**, *18* (47), 6951−6959.
(16) Moohammadaree, A.; Changtam, C.; Wicha, P.; Suksamrarn, A.; Tocharus, J.; Tocharus, C. Mechanisms of vasorelaxation induced by hexahydrocurcuminin isolated rat thoracic aorta. *Phytother. Res.* **2015**, *29* (11), 1806−1813.
(17) Wicha, P.; Tocharus, J.; Janyou, A.; Jittiwat, J.; Chaichompoo, W.; Suksamrarn, A.; Tocharus, C. Hexahydrocurcumin alleviated blood-brain barrier dysfunction in cerebral ischemia/reperfusion rats. *Pharmacol. Rep.* **2020**, *72* (3), 659−671.
(18) Jearjaroen, P.; Pakdeepak, K.; Tocharus, C.; Chaichompoo, W.; Suksamrarn, A.; Tocharus, J. Inhibitory effect of hexahydrocurcumin on memory impairment and amyloidogenesis in dexamethasone-treated mice. *Neurotoxic. Res.* **2021**, *39*, 266−276.
(19) Jearjaroen, P.; Thangwong, P.; Tocharus, C.; et al. Hexahydrocurcumin attenuated demyelination and improved cognitive impairment in chronic cerebral hypoperfusion rats. *Inflammopharmacology* **2024**, *32*, 1531−1544.
(20) Panthiya, L.; Tocharus, J.; Onsa-Ard, A.; Chaichompoo, W.; Suksamrarn, A.; Tocharus, C. Hexahydrocurcumin ameliorates hypertensive and vascular remodeling in L-NAME-induced rats. *Biochim. Biophys. Acta, Mol. Basis Dis.* **2022**, *1868* (3), No. 166317.
(21) Jude, S.; Amalraj, A.; Kunnumakkara, A. B.; Divya, C.; Löffler, B. M.; Gopi, S. Development of validated methods and quantification of curcuminoids and curcumin metabolites and their pharmacokinetic study of oral administration of complete natural turmeric formulation (Cureit) in human plasma via UPLC/ESI-Q-TOF-MS spectrometry. *Molecules* **2018**, *23* (10), 2415.
(22) Zheng, Y.; Xu, J.; Ma, G.; Zhang, J.; Zhu, Q.; Liu, H.; Zhang, P.; Zhu, Y.; Cai, W. Bioavailability and pharmacokinetics of S-propargyl-L-cysteine, a novel cardioprotective agent, after single and multiple doses in Beagle dogs. *Xenobiotica* **2012**, *42* (3), 304−309.
(23) Vareed, S. K.; Kakarala, M.; Ruffin, M. T.; Crowell, J. A.; Normolle, D. P.; Djuric, Z.; Brenner, D. E. Pharmacokinetics of curcumin conjugate metabolites in healthy human subjects. *Cancer Epidemiol., Biomarkers Prev.* **2008**, *17* (6), 1411−1417.
(24) Heger, M.; van Golen, R. F.; Broekgaarden, M.; Michel, M. C. The Molecular basis for the pharmacokinetics and pharmacodynamics of curcumin and its metabolites in relation to cancer. *Pharmacol. Rev.* **2014**, *66* (1), 222−307.
(25) Shi, M.; Gao, T.; Zhang, T.; Han, H. Characterization of curcumin metabolites in rats by ultra-high-performance liquid chromatography with electrospray ionization quadrupole time-of-flight tandem mass spectrometry. *Rapid Commun. Mass Spectrom.* **2019**, *33* (13), 1114−1121.
(26) Yang, K. Y.; Lin, L. C.; Tseng, T. Y.; Wang, S. C.; Tsai, T. H. Oral bioavailability of curcumin in rat and the herbal analysis from Curcuma longa by LC-MS/MS. *J. Chromatogr. B: Anal. Technol. Biomed. Life Sci.* **2007**, *853* (1−2), 183−189.
(27) Pan, M. H.; Huang, T. M.; Lin, J. K. Biotransformation of curcumin through reduction and glucuronidation in mice. *Drug Metab. Dispos.* **1999**, *27* (4), 486−494.
(28) Marczylo, T. H.; Steward, W. P.; Gescher, A. J. Rapid analysis of curcumin and curcumin metabolites in rat biomatrices using a novel ultraperformance liquid chromatography (UPLC) method. *J. Agric. Food Chem.* **2009**, *57* (3), 797−803.
(29) Wang, J.; Yu, X.; Zhang, L.; Wang, L.; Peng, Z.; Chen, Y. The pharmacokinetics and tissue distribution of curcumin and its metabolites in mice. *Biomed. Chromatogr.* **2018**, *32* (9), No. e4267.
(30) Verma, M. K.; Najar, I. A.; Tikoo, M. K.; Singh, G.; Gupta, D. K.; Anand, R.; Khajuria, R. K.; Sharma, S. C.; Johri, R. K. Development of a validated UPLC-qTOF-MS method for the determination of curcuminoids and their pharmacokinetic study in mice. *Daru, J. Pharm. Sci.* **2013**, *21* (1), No. 11.
(31) Al Shoyaib, A.; Archie, S. R.; Karamyan, V. T. Intraperitoneal Route of Drug Administration: Should it Be Used in Experimental Animal Studies? *Pharm. Res.* **2020**, *37* (1), No. 12.
(32) Szymusiak, M.; Hu, X.; Plata, P. A. L.; Ciupinski, P.; Wang, Z. J.; Liu, Y. Bioavailability of curcumin and curcumin glucuronide in the central nervous system of mice after oral delivery of nano-curcumin. *Int. J. Pharm.* **2016**, *511* (1), 415−423.
(33) Bučević Popović, V.; Karahmet Farhat, E.; Banjari, I.; Jeličić Kadić, A.; Puljak, L. Bioavailability of Oral Curcumin in Systematic Reviews: A Methodological Study. *Pharmaceuticals* **2024**, *17*, 164.
(34) Gutierres, V. O.; Campos, M. L.; Arcaro, C. A.; Assis, R. P.; Baldan-Cimatti, H. M.; Peccinini, R. G.; Paula-Gomes, S.; Kettelhut, I. C.; Baviera, A. M.; Brunetti, I. L. Curcumin Pharmacokinetic and Pharmacodynamic Evidences in Streptozotocin-Diabetic Rats Support the Antidiabetic Activity to Be via Metabolite(s). *J. Evidence-Based Complementary Altern. Med.* **2015**, *2015*, No. 678218.
(35) Changtam, C.; de Koning, H. P.; Ibrahim, H.; Sajid, M. S.; Gould, M. K.; Suksamrarn, A. Curcuminoid analogs with potent

https://doi.org/10.1021/acsomega.4c06604
ACS Omega 2024, 9, 41032−41042

activity against Trypanosoma and Leishmania species. *Eur. J. Med. Chem.* **2010**, *45* (3), 941−956.
(36) USFDA. Bioanalytical Method Validation Guidance for Industry, 2018. https://www.fda.gov/regulatory-information/search-fda-guidance-documents/bioanalytical-method-validation-guidance-industry.

https://doi.org/10.1021/acsomega.4c06604
ACS Omega 2024, 9, 41032−41042